Summary of Recent Improvements and Applications of CFD-Based Aeroelastic Reduced-Order Models

Walter A. Silva *
NASA Langley Research Center
Hampton, Virginia 23681-0001

Recent enhancements to the development of CFD-based unsteady aerodynamic and aeroelastic reduced-order models (ROMs) are presented. These enhancements include the simultaneous application of structural modes as CFD input, static aeroelastic analysis using a ROM, and matched-point solutions using a ROM. The simultaneous application of structural modes as CFD input enables the computation of the unsteady aerodynamic state-space matrices with a single CFD execution, independent of the number of structural modes. The responses obtained from a simultaneous excitation of the CFD-based unsteady aerodynamic system are processed using system identification techniques in order to generate an unsteady aerodynamic state-space ROM. Once the unsteady aerodynamic state-space ROM is generated, a method for computing the static aeroelastic response using this unsteady aerodynamic ROM and a state-space model of the structure, is presented. Finally, a method is presented that enables the computation of matched-point solutions using a single ROM that is applicable over a range of dynamic pressures and velocities for a given Mach number. These enhancements represent a significant advancement of unsteady aerodynamic and aeroelastic ROM technology.

Introduction

THE goal behind the development of reduced-order models (ROMs) for computational aeroelasticity is aimed at addressing two primary challenges: reducing computational cost and enabling the use of CFD information by other disciplines. Development of a ROM entails the creation of a simplified mathematical model that captures the dominant dynamics of the original system. The simplicity of the ROM yields significant improvements in computational efficiency as compared to the original system, thereby addressing the first challenge. This simplified mathematical representation of the original system is, by design, in a mathematical form suitable for use in a multidisciplinary, preliminary design environment. As a result, interconnection of the ROM with other disciplines is possible, thereby addressing the second challenge.

Silva and Bartels[1] presented the development of linearized, unsteady aerodynamic state-space models for prediction of flutter and aeroelastic response using the parallelized, aeroelastic capability of the CFL3Dv6.0 code. The results presented provided an important validation of the various phases of the ROM development process. The Eigensystem Realization Algorithm (ERA),[2] which transforms an impulse response into state-space form, was applied for the development of the aerodynamic state-space models. Flutter results for the AGARD 445.6 Aeroelastic Wing using the CFL3Dv6.0 code were presented as well, including computational costs. Unsteady aerodynamic state-space models were generated and coupled with a state-space model of the structure within a MATLAB/SIMULINK[3] environment for rapid calculation of aeroelastic responses including flutter. Aeroelastic responses computed directly using the CFL3Dv6.0 code showed excellent comparison with the aeroelastic responses computed using the CFD-based ROM within the MATLAB/SIMULINK environment.

The aerodynamic impulse responses that were used to generate the unsteady aerodynamic ROM for the AGARD wing were computed using CFL3Dv6.0 via the excitation of one mode at a time. The one-mode-at-a-time method is referred to as the Original ROM approach. For a four-mode system such as the AGARD wing, these one-mode-at-a-time computations were not very expensive. However, for more realistic cases where the number of modes can be an order of magnitude or more larger, the one-mode-at-a-time method becomes impractical. Kim et al[4] have proposed methods that enable the simultaneous application of structural modes as CFD input, greatly reducing the cost of identifying the aerodynamic impulse responses from the CFD code. Kim's method

*Senior Research Scientist, Aeroelasticity Branch, NASA Langley Research Center, Hampton, Virginia; AIAA Associate Fellow

consists of using simultaneous staggered step inputs, one per mode, and then recovering the individual responses from this simultaneous excitation.

In another paper,[5] three new types of input functions are introduced that can be used to simultaneously apply the structural modes to the CFD code while enabling the recovery of the individual responses. This new capability will enable the computation of aerodynamic impulse responses for any number of structural modes using a single CFD execution. Reduced-order models generated using the one-mode-at-a-time method are compared to ROMs using the simultaneous excitation inputs. The present paper will provide a brief overview of this new capability.

In addition, a new method for computing static aeroelastic solutions using ROMs is presented. Previously, ROMs were generated about a static aeroelastic condition computed using the CFD code. The applicability of the ROM about that condition was limited to a small range of dynamic pressures that would not deviate too far from the static aeroelastic condition. This limitation also applies to the method presented by Kim et al.[4] The method presented by Raveh[6] was applied to the AGARD wing. At zero degrees angle of attack and with a symmetric airfoil shape, this wing does not induce a static aeroelastic response. It is not stated in the reference by Raveh[6] how that method should be applied to a configuration that includes static aeroelastic effects. With this new capability to use the ROM for computing the static aeroelastic solution, there is no need to compute a separate static aeroelastic solution using the CFD code, thereby improving computational efficiency.

Finally, a new method for computing matched-point aeroelastic solutions without re-execution of the CFD code is presented as well. This new matched-point solution method extends the applicability of a single ROM to include velocity variations in addition to changes in dynamic pressure in order to simulate a true flight condition (Mach number, velocity, and dynamic pressure).

Description of the CFD and System Identification Methods

The following subsections describe the parallelized, aeroelastic version of the CFL3Dv6.4 code and the system identification methods employed in the development of a ROM.

CFL3Dv6.4 Code

The computer code used in this study is the CFL3Dv6.4 code, which solves the three-dimensional, thin-layer, Reynolds averaged Navier-Stokes equations with an upwind finite volume formulation.[7–9] The code uses third-order upwind-biased spatial differencing for the inviscid terms with flux limiting in the presence of shocks. Either flux-difference splitting or flux-vector splitting is available. The flux-difference splitting method of Roe[10] is employed in the present computations to obtain fluxes at cell faces. There are two types of time discretization available in the code. The first-order backward time differencing is used for steady calculations while the second-order backward time differencing with subiterations is used for static and dynamic aeroelastic calculations. Furthermore, grid sequencing for steady state and multigrid and local pseudo-time stepping for time marching solutions are employed.

One of the important features of the CFL3Dv6.4 code is its capability of solving multiple zone grids with one-to-one connectivity. Spatial accuracy is maintained at zone boundaries, although subiterative updating of boundary information is required. Coarse-grained parallelization using the Message Passing Interface (MPI) protocol can be utilized in multiblock computations by solving one or more blocks per processor. When there are more blocks than processors, optimal performance is achieved by allocating an equal number of grid points to each processor. As a result, the time required for a CFD-based aeroelastic computation can be dramatically reduced.

Because the CFD and computational structural mechanics (CSM) meshes usually do not match at the interface, CFD/CSM coupling requires a surface spline interpolation between the two domains. The interpolation of CSM mode shapes to CFD surface grid points is done as a preprocessing step. Modal deflections at all CFD surface grids are first generated. Modal data at these points are then segmented based on the splitting of the flow field blocks. Mode shape displacements located at CFD surface grid points of each segment are used in the integration of the generalized modal forces and in the computation of the deflection of the deformed surface. The final surface deformation at each time step is a linear superposition of all the modal deflections.

System/Observer/Controller Identification Toolbox (SOCIT)

In structural dynamics, the realization of discrete-time state-space models that describe the modal dynamics of a structure has been enabled by the development of algorithms such as the Eigensystem Realization Algorithm (ERA)[2] and the Observer Kalman Identification (OKID)[11] Algorithm. These algorithms perform state-space realizations by using the Markov parameters (discrete-time impulse responses) of the systems of interest. These algorithms have been combined into one package known as the System/Observer/Controller Identification Tool-

box (SOCIT)[12] developed at NASA Langley Research Center.

The first phase of the ROM development process is the identification of the individual impulse responses for each input/output combination. The PULSE algorithm is used to extract these individual input/output impulse responses from simultaneous input/output responses. For a four-input/four-output system, simultaneous application of all four inputs[5] yields four output responses. The PULSE algorithm is used to extract the individual sixteen (four times four) impulse responses that associate the response in one of the outputs due to one of the inputs. Details of the PULSE algorithm are provided in the references.

For the second phase of the ROM development process, once the individual sixteen impulse responses are available, they are then processed via the Eigensystem Realization Algorithm (ERA) in order to transform the sixteen individual impulse responses into a four-input/four-output, discrete-time, state-space model. A brief summary of the basis of this algorithm follows.

A finite dimensional, discrete-time, linear, time-invariant dynamical system has the state-variable equations

$$x(k+1) = Ax(k) + Bu(k) \tag{1}$$

$$y(k) = Cx(k) + Du(k) \tag{2}$$

where x is an n-dimensional state vector, u an m-dimensional control input, and y a p-dimensional output or measurement vector with k being the discrete time index. The transition matrix, A (n x n), characterizes the dynamics of the system. The goal of system realization is to generate constant matrices (A, B, C) such that the output responses of a given system due to a particular set of inputs is reproduced by the discrete-time state-space system described above.

For the system of Eqs. (1) and (2), the time-domain values of the systems discrete-time impulse response are also known as the Markov parameters and are defined as

$$Y(k) = CA^{k-1}B \tag{3}$$

with B an (n x m) matrix and C a (p x n) matrix. The ERA algorithm begins by defining the generalized Hankel matrix consisting of the discrete-time impulse responses for all input/output combinations. The algorithm then uses the singular value decomposition (SVD) to compute the A, B, and C matrices.

In this fashion, the ERA is applied to unsteady aerodynamic impulse responses to construct unsteady aerodynamic state-space models.

Original ROM Development Processes

A CFD-based aeroelastic system can be viewed as the coupling of a nonlinear unsteady aerodynamic system (flow solver) with a structural system as depicted in Figure 1. The present study focuses on the development of a linearized unsteady aerodynamic ROM (in state-space form), using the general procedure depicted in Figure 2, that is then coupled to a structural model (also in state-space form) for aeroelastic analyses. For the discussions that follow, the term ROM will refer to the unsteady aerodynamic state-space model. When the unsteady aerodynamic state-space model (ROM) is connected to a state-space model of the structure within the SIMULINK environment, this system is often also referred to as a ROM. However, to avoid confusion, the SIMULINK aeroelastic system will be referred to as the aeroelastic simulation ROM.

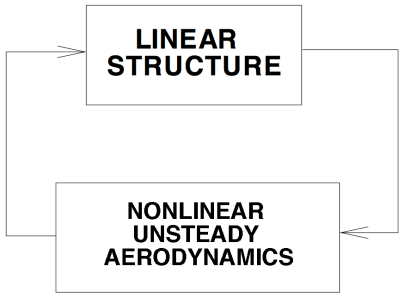

Fig. 1 Coupling of structure and aerodynamics within an aeroelastic CFD code.

An outline of the original (one-mode-at-a-time) ROM development process[1] is presented as background for the new enhancements. The original ROM development process is as follows:

1. Implementation of impulse/step response technique into aeroelastic CFD code;
2. Computation of impulse/step responses for each mode, one mode at a time, of an aeroelastic system using the aeroelastic CFD code; these responses are computed about a static aeroelastic solution (or a given dynamic pressure);
3. Impulse responses generated in Step 2 are transformed into an unsteady aerodynamic state-space system using the ERA (within SOCIT);
4. Evaluation/validation of the state-space models generated in Step 3 via comparison with CFD results (i.e., ROM results vs. full CFD solution results);

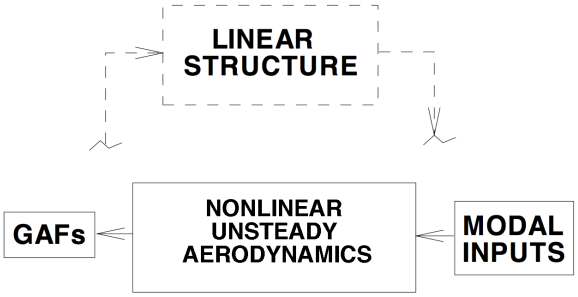

Fig. 2 Identification of generalized aerodynamic forces (GAFs).

In the original ROM process, since each mode is being excited individually, the response in each output due to a particular input (e.g., the impulse response in output 2 due to input 1) is generated almost directly. If the function being used to excite the system is an impulse (or a unit pulse for discrete-time systems), then the output from the CFD solution will consist of the impulse response of each output due to that one input. If the function being used to excite the system is not an impulse function (such as a step input or a random input), then the impulse response needs to be extracted from the input/output data. One method for extraction is deconvolution[1] but there are other methods that can be used. For the original ROM process, since each input to a system is being excited individually, the exact nature of the input function is defined, to a certain extent, based on user preference (frequency range of interest, ease of implementation into a CFD solver, etc.). The step input has emerged as a convenient input for the original ROM process due to its ease of implementation into a CFD solver and to the wide range of frequency excitation that it can generate.

The primary issue,then, with the original ROM process was the identification of the unsteady aerodynamic impulse responses one mode at a time (Step 2). Clearly, for a large number of modes, this procedure becomes impractical.

Improved ROM Development Processes

An outline of the improved simultaneous modal excitation ROM development process with the recent enhancements is as follows:

1. Generate the number of functions (from a selected family) that corresponds to the number of structural modeshapes;

2. Apply the generated input functions simultaneously via one CFD execution; these responses are computed directly from the restart of a steady rigid CFL3D solution (not about a particular dynamic pressure);

3. Using the simultaneous input/output responses, identify the individual impulse responses using the PULSE algorithm (within SOCIT);

4. Transform the individual impulse responses generated in Step 3 into an unsteady aerodynamic state-space system using the ERA(within SOCIT);

5. Evaluate/validate the state-space models generated in Step 4 via comparison with CFD results (i.e., ROM results vs. full CFD solution results);

An important difference between the original ROM process and the improved ROM process is stated in steps (2) of the outlines above. For the original ROM process, if a static aeroelastic condition existed, then a ROM was generated about a selected static aeroelastic condition. So a static aeroelastic condition of interest was defined (typically a dynamic pressure) and that static aeroelastic condition was computed using CFL3D as a restart from a converged steady, rigid solution. Once a converged static aeroelastic solution was obtained, the ROM process was applied about that condition. This implies that the resultant ROM is, of course, limited in some sense to the neighborhood of that static aeroelastic condition. Moving "too far away" from that condition could result in loss of accuracy.

The reason for generating ROMs in this fashion was because no method had been defined to enable the computation of a static aeroelastic solution using a ROM. Any ROMs generated in this fashion were, therefore, limited to the prediction of dynamic responses about a static aeroelastic solution including the methods by Raveh[6] and by Kim et al.[4] The improved ROM method, however, includes a method for generating a ROM directly from a steady, rigid solution. As a result, these improved ROMs can then be used to predict both static aeroelastic and dynamic solutions for any dynamic pressure. In order to capture a specific range of aeroelastic effects (previously obtained by selecting a particular dynamic pressure), the improved ROM method relies on the excitation amplitude to excite aeroelastic effects of interest. The details of the method for using a ROM for computing both static aeroelastic and dynamic solutions is presented in another reference by the present author.[13] For the present results, all responses were computed from the restart of a steady, rigid CFL3D solution, bypassing the need (and additional computational expense) to execute a static aeroelastic solution using

CFL3D.

Simultaneous Excitation Input Functions

In the situation where the goal is the simultaneous excitation of a multiple-input multiple-output (MIMO) system, system identification techniques[14–16] dictate that the nature of the input functions used to excite the system must be properly defined if accurate input/output models of the system are to be generated. The most important point to keep in mind when defining these input functions is that these functions need to be different, in some sense, from each other. This makes sense since, if the excitation inputs are identical and they are applied simultaneously, it becomes practically impossible for any system identification algorithm to relate the effects of one input on a given output. This, in turn, makes it practically impossible for that algorithm to extract the individual impulse responses for each input/output pair. As has already been well established, the individual impulse responses for each input/output pair are necessary ingredients towards the development of state-space models. With respect to unsteady aerodynamic MIMO systems, these individual impulse responses correspond to time-domain generalized aerodynamic forces (GAFs), critical to understanding unsteady aerodynamic behavior. The Fourier-transformed version of these GAFs are the frequency-domain GAFs which provide an important link to more traditional frequency-domain-based aeroelastic analyses.

The question is how different should these input functions be and how can we quantify a level of "difference" between each input function? Kim[4] uses the familiar step function as the input function but with each step input being applied at a different point in time (lagged) in order to maintain some difference between the input signals. Kim refers to this family of lagged step functions as "almost orthogonal". As Kim points out, the greater the lag between successive step inputs, the greater the difference between input signals. This then presents a spectrum of possibilities where, at one end, one has step input functions with no lags (identical functions, not orthogonal) and at the other end the step functions are separated by an extremely large lag (in the limit, these are the individual step inputs from the original ROM process). Since orthogonality (linear independence) is the most precise mathematical method for guaranteeing the "difference" between signals, the present research focuses on the application of families of orthogonal functions as candidate input functions. Using orthogonal functions directly provides a mathematical guarantee that the input functions are as different as mathematically possible. These orthogonal input functions then can be considered optimal input functions for the identification of a MIMO system.

In the paper by Silva,[5] four families of functions were applied towards the efficient identification of a CFD-based unsteady aerodynamic state-space model: lagged step, block pulse, Haar, and Walsh. Although it has been stated by Kim that the lagged-step functions are not completely orthogonal (almost orthogonal), these functions are used in the present study for comparison purposes. The other three functions each represent an orthogonal family of functions. The block pulse functions, presented in Figure 3, are orthogonal and resemble a modified step input. An advantage of step-like functions is the broad frequency bandwidth that is excited by the impulsive nature of these functions. An added benefit of the block pulse functions over traditional step functions is that block pulse inputs provide excitation to the system in both positive and negative directions. From an unsteady aerodynamics point of view, it is important that modes of realistic wing configurations (e.g., with a non-symmetric airfoil) be excited in both directions for a more complete capture of relevant dynamics. For the present paper, results will be limited to the application of Walsh functions with a limited overview of the other functions.

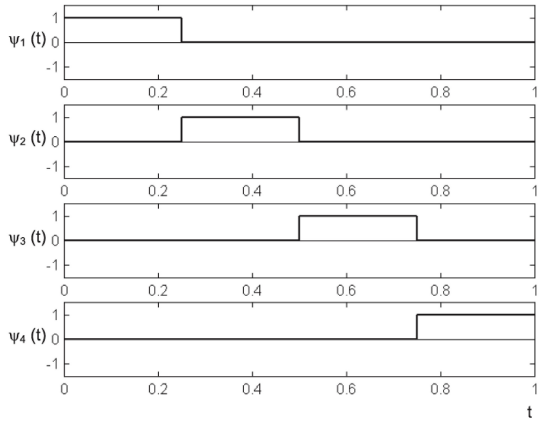

Fig. 3 Block pulse functions.

The Haar functions, presented in Figure 4, comprise one of the simplest form of wavelet functions. These functions are orthogonal by the mathematical definition of wavelet functions. Likewise, this family of functions has a similarity to step inputs and therefore embodies the impulsive (i.e., beneficial) nature of step inputs with regards to frequency bandwidth. The final set of orthogonal functions is the Walsh function, presented in Figure 5.

It is important to mention that the Haar functions are generated using formulas based on a power of two algorithm. These functions have yielded excellent

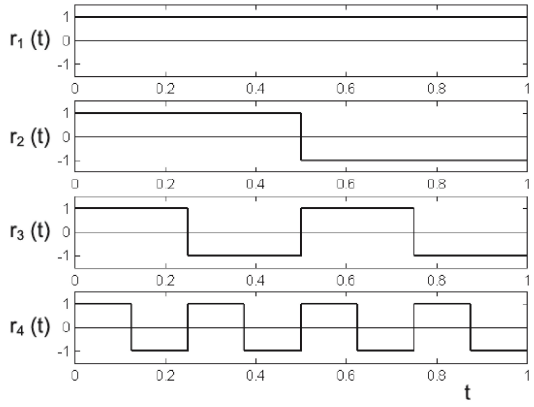

Fig. 4 Haar (wavelet) functions.

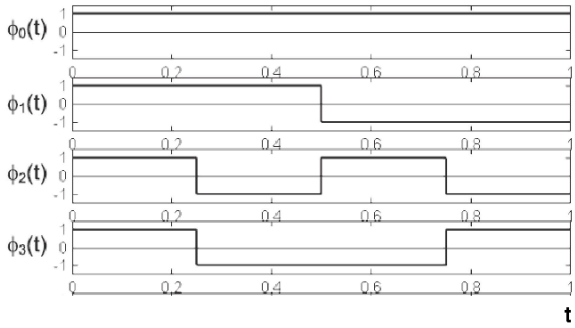

Fig. 5 Walsh functions.

results when applied towards the identification of a CFD-based unsteady aerodynamic state-space model using a single CFL3D execution for a multi-mode configuration. However, due to the fact that these functions are generated based on a power of two algorithm, the number of modes drives the size and, subsequently, the record length of the input functions that are then input to CFL3D. As a result, this can severely limit the number of modes that can be excited at one time. For example, if ten modes are to be excited simultaneously, then the record length of the ten Haar functions generated (one per mode) is defined by the record length of the Haar function that corresponds to mode ten. Then taking two to the power of ten yields 1024 time steps. Twelve modes yields a record length for the Haar functions of 4096 time steps, thirteen modes yields 8192 time steps, fourteen modes yields 16384 time steps, and so on. Clearly, for a very large number of modes, this family of functions is not practical. Therefore, Silva[5] presented only those results for the lagged step (not orthogonal), the block pulse (orthogonal), and the Walsh (orthogonal) functions. For the present paper, results will be limited to application of the Walsh functions.

Supersonic Semi-Span CFD Model

The configuration used for the present analyses is a supersonic semi-span wind-tunnel model known as the Rigid Semi-span Model (RSM). This configuration has been tested several times at the NASA Langley's Transonic Dynamics Tunnel (TDT). The actual wind-tunnel model was fabricated using graphite and is very rigid. However, as part of collaborative studies between the NASA Langley Research Center and the Boeing Company (Seattle), a "softened" computational model of the RSM was developed by Dr. Moeljo Hong (Boeing).[17] The model was "softened" by simply reducing the four modal frequencies by a factor of four.

The results presented are for Euler (inviscid)solutions at a Mach number of 0.7 and an angle of attack of 3 degrees. This configuration does not have a symmetric airfoil and will, therefore, generate a static aeroelastic response in addition to the dynamic aeroelastic response. The method for using an unsteady aerodynamic state-space ROM for static aeroelastic responses is not presented in this paper but is presented in another paper by this author.[13] Figure 6 presents the surface grid for the CFL3D RSM configuration.

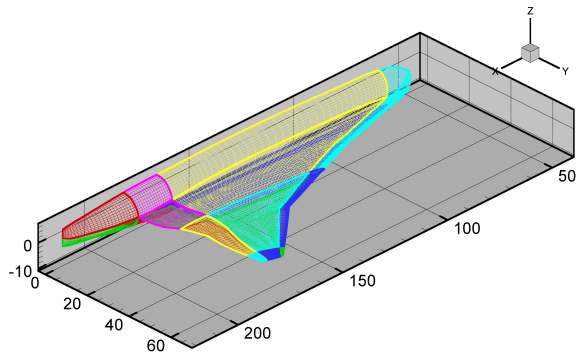

Fig. 6 Computational grid of supersonic semi-span configuration.

Simultaneous Excitation Results

In Figure 7, Figure 8, Figure 9, and Figure 10 each of the four Walsh functions is presented separately for clarity. The CFL3D response in the first generalized coordinate due to the Walsh function inputs is presented in Figure 11. The Walsh functions were generated over a record length of 2000 time steps.

Processing the outputs for all four generalized coordinates for each input function through the PULSE algorithm in SOCIT, the time-domain generalized aerodynamic forces (GAFs) can be identified.

Additional comparison of these results can be obtained via the analysis of the frequency-domain version of the GAFs. The frequency-domain GAFs are compared to the frequency-domain GAFs from the use

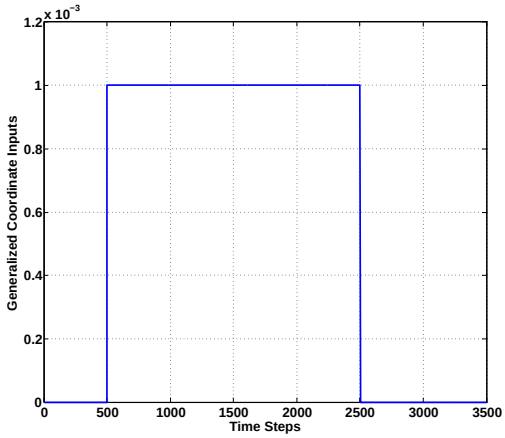

Fig. 7 Walsh input function for the first mode (shown separately).

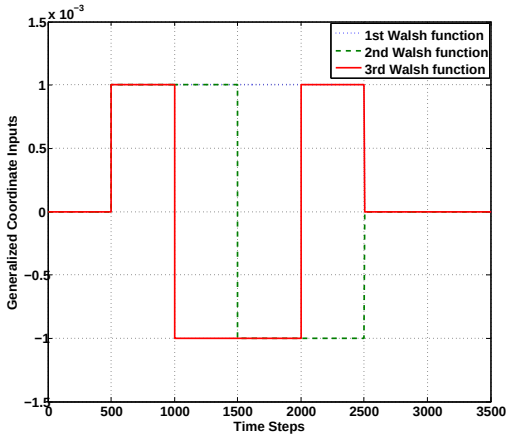

Fig. 9 Walsh input function for the first, second, and third modes.

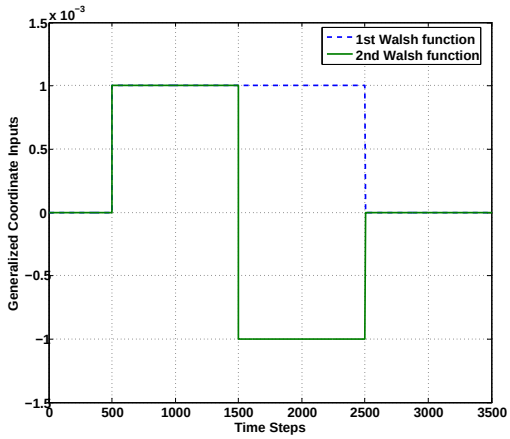

Fig. 8 Walsh input function for the first and second modes.

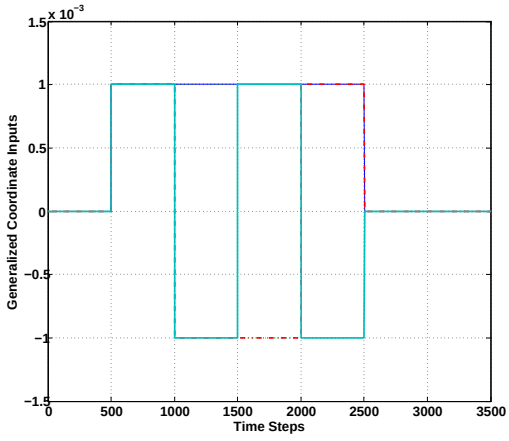

Fig. 10 Walsh input function for the first, second, third, and fourth modes.

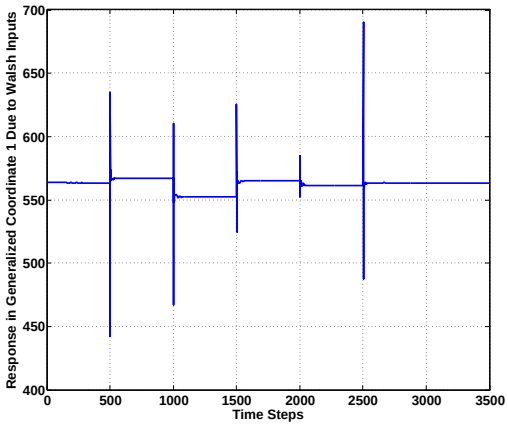

Fig. 11 CFL3D response in the first generalized coordinate due to excitation using Walsh functions.

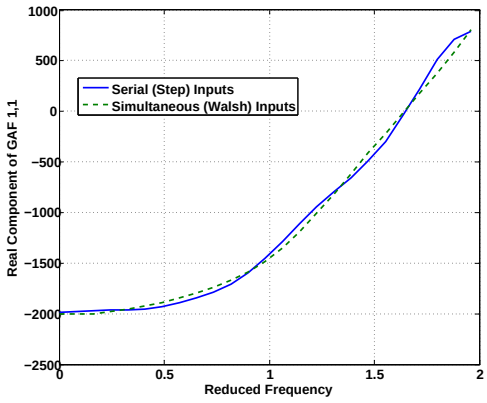

Fig. 12 Real component of GAF 1,1 for the Walsh and serial step inputs.

of serial (one-at-a-time) step inputs. Comparison of the simultaneous input responses with those from the one-mode-at-a-time does not imply that the one-mode-at-a-time results are the correct results. That is, it is quite possible that (and most probable) that the responses obtained from the simultaneous excitation will be different from the responses obtained from the one-mode-at-a-time excitations due to potential nonlinear modal coupling effects. The reason for comparing these two sets of responses is simply due to the fact that the one-mode-at-a-time responses represent the original ROM approach. Application of an FFT to each one of the time-domain GAFs directly yields the desired frequency-domain GAFs.[1] Only a subset of the sixteen GAFs will be presented in the figures below.

The real and imaginary components of GAF 1,1 due to the Walsh function inputs are presented as Figure 12 and Figure 13. For both the real and imaginary components, once again, noticeable improvement in the comparison is achieved with the use of the Walsh function. In particular, for both the block pulse and the Walsh functions, the steady value (value at zero reduced frequency) is well captured.

Figure 14 and Figure 15 are the comparison of the real and imaginary components of GAF 2,2 for the Walsh and the serial (step) inputs. An improvement in the comparison is once again noted.

The time-domain GAFs are then processed through the ERA (part of SOCIT) in order to generate a state-space model of the unsteady aerodynamic system. The

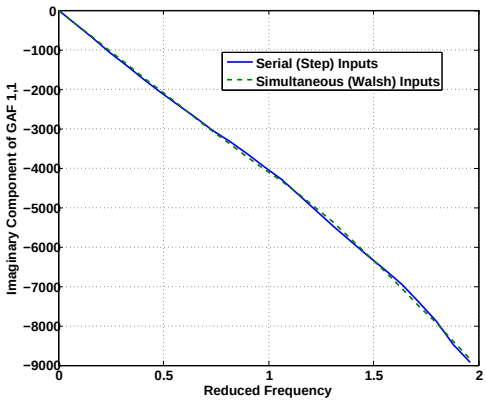

Fig. 13 Imaginary component of GAF 1,1 for the Walsh and serial step inputs.

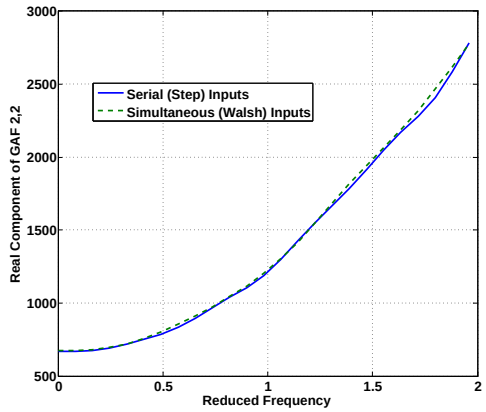

Fig. 14 Real component of GAF 2,2 for the Walsh and serial step inputs.

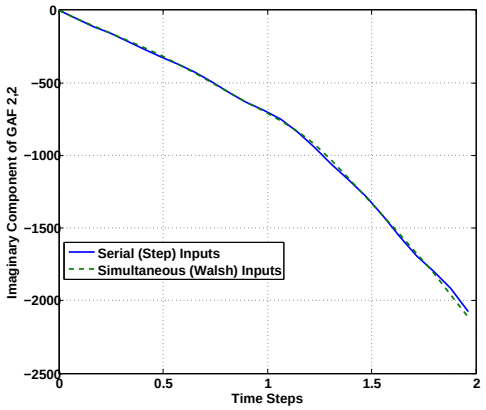

Fig. 15 Imaginary component of GAF 2,2 for the Walsh and serial step inputs.

resultant state-space models (for the lagged step with 50 time-step delays and the Walsh functions) were 12th order in dimension. To demonstrate the effectiveness of the new input functions, a representative result is presented as Figure 16, a comparison of responses in the four generalized coordinates for the CFL3D solution and the ROM solution. The CFL3D responses are from a CFL3D solution that includes both static and dynamic aeroelastic responses simultaneously. Typically, static and dynamic aeroelastic responses are computed separately in order to reduce computational cost. A static aeroelatic solution is computed as the restart solution from a steady, rigid solution using an artifically high structural damping value in order to accelerate convergence to a static aeroelastic solution. Then, a dynamic aeroelastic solution is computed as the restart solution from the converged static aeroelastic solution. In the paper by the present author,[13] a method is introduced that enables the prediction of static and dynamic aeroelastic solutions from the same ROM. For the present paper, the sample results presented in Figure 16 are for a full solution; that is, a solution that includes both static and dynamic responses for a given dynamic pressure. In this case, the results presented are for a dynamic pressure of 0.1 psi. Notice that the solutions start at a generalized coordinate value of zero (static, rigid solution) and converge to a non-zero mean value (static aeroelastic solution) with the dynamic solution superimposed on the static solution. As can be seen, the comparison is very good and the ROM captures the combined static and dynamic aeroelastic responses predicted by the CFL3D solution.

Static/Dynamic Aeroelastic CFD-Based Analyses

Traditional Approach

The configuration used for this section of the paper is the supersonic semi-span wind-tunnel model known as the Rigid Semi-span Model (RSM) previously mentioned. The traditional process for generating CFD-based aeroelastic responses consists of three steps: 1). perform computation of a converged steady, rigid solution at a given Mach number and angle of attack; 2). at the same Mach number and angle of attack, perform computation of a converged static aeroelastic solution at a selected dynamic pressure and velocity; 3). at the same Mach number, angle of attack, dynamic pressure, and velocity, perform computation of a dynamic aeroelastic response. A sketch depicting this process is presented as Figure 17. This method was applied successfully by Silva and Bennett[18] for prediction of the aeroelastic responses of the Active Flexible Wing (AFW) wind-tunnel model.

The static aeroelastic solution is computed by

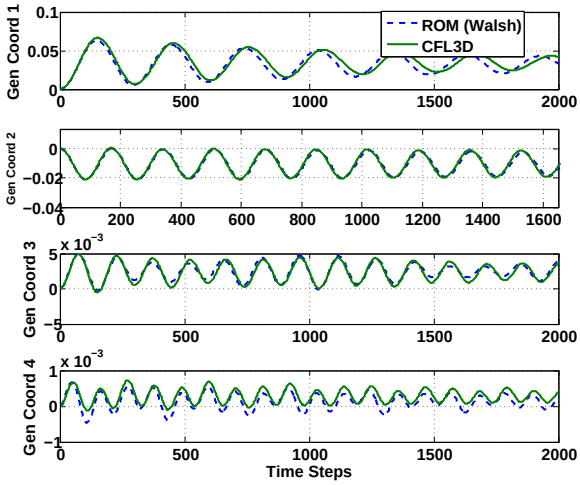

Fig. 16 Full solution (static plus dynamic aeroelastic responses) generalized coordinate responses at a dynamic pressure of 0.1 psi.

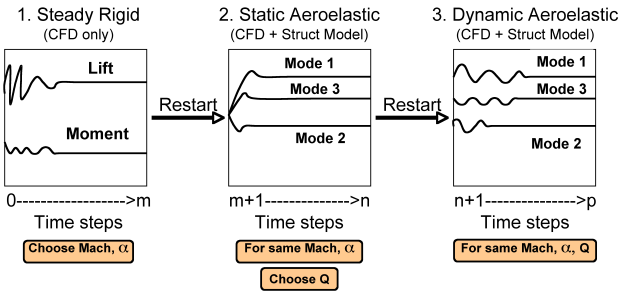

Fig. 17 Sketch depicting the traditional process for generating CFD-based aeroelastic responses.

restarting the converged steady, rigid solution. The converged steady, rigid solution, therefore serves as the initial condition for the static aeroelastic solution. Likewise, the converged static aeroelastic solution serves as the initial condition for the dynamic aeroelastic solution. The static aeroelastic solution is computed by imposing a very large value of modal damping to the system, thereby attenuating dynamic transients and yielding static aeroelastic deflections. In addition, the initial conditions (initial generalized displacements and velocities) are set to zero within the structural integrator portion of CFL3D. An example of a static aeroelastic solution for the softened RSM configuration is presented as Figure 18 where the artificially-excessive modal damping (0.99) results in an acceleration of the static aeroelastic convergence by attenuating dynamic transients.

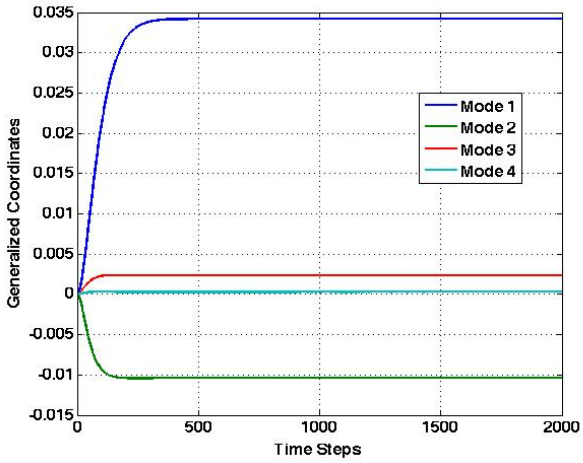

Fig. 18 Converged static aeroelastic solution for the RSM configuration at 0.7 Mach number, 3 degrees angle of attack, and 0.1 psi dynamic pressure.

Upon achieving a converged static aeroelastic solution, a dynamic solution is computed by restarting the static aeroelastic solution. The restarting of a solution file basically defines the initial structural and flow conditions from the previous solution (the static aeroelastic solution in this case). For the dynamic solution, the value of modal damping is set to a realistic value (typically zero or on the order of 1-3 percent of critical). The initial conditions of the structure are now set to non-zero values in order to provide an initial excitation to the system. Typically, generalized velocities are set to some small value while the generalized displacements are set to zero. The resultant dynamic aeroelastic solution for zero modal damping and a value of 0.001 for all four generalized velocities is presented as Figure 19. Zooming in on the first generalized coordinate, presented as Figure 20, the stability of the dynamic response can be ascertained. However, post-processing of the generalized aerodynamic transients is required to obtain damping and frequency estimates.

The primary reason for performing separate and serial static and dynamic aeroelastic solutions[18] was for computational efficiency, as follows. Clearly, a solution can be obtained which contains both the static and dynamic solutions occurring simultaneously by setting modal damping to zero (or a small value), setting the structural initial conditions (generalized velocities) to small non-zero values, and restarting this combined solution from the restart file of a converged steady, rigid

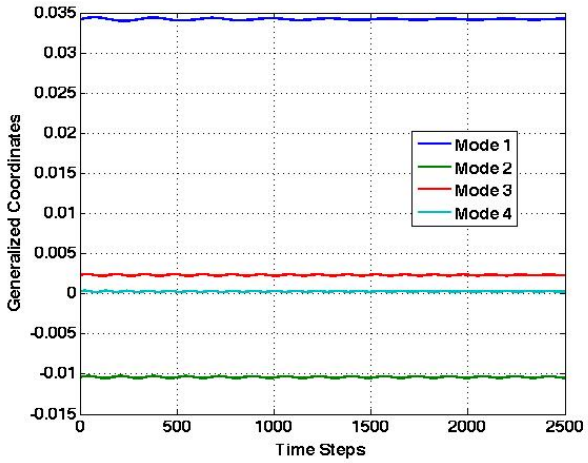

Fig. 19 Dynamic aeroelastic response for the RSM configuration at 0.7 Mach number, 3 degrees angle of attack, and 0.1 psi dynamic pressure about the converged static aeroelastic response at the same conditions.

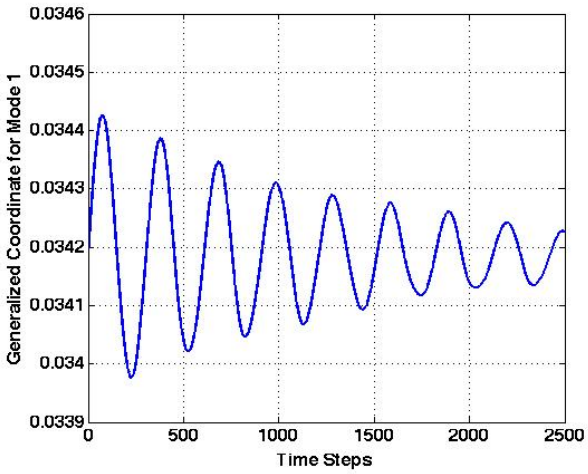

Fig. 20 Blow up of the first mode dynamic aeroelastic response from Figure 19.

solution. A combined solution for a dynamic pressure of 0.1 psi is presented as Figure 21.

For some configurations, when performing a combined solution, the convergence of the static portion of the response could require a large number of time steps, making it difficult to clearly define the dynamic portion of the response (stability). Therefore, in separating the solution process and artificially accelerating the static aeroelastic solution, that portion of the computational cost can be reduced. Then, the dynamic solution can be generated without the added effect of a static variation and, subsequently, may be easier to interpret. However, this process may need to be revisited for complex configurations to determine

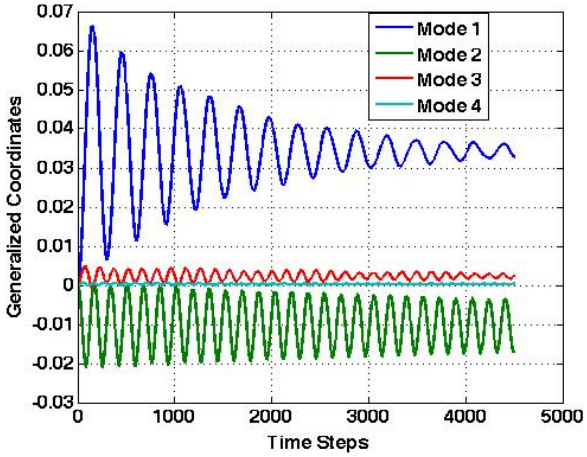

Fig. 21 Combined CFL3D aeroelastic solution that includes static and dynamic solutions simultaneously for the RSM configuration at 0.7 Mach number, 3 degrees angle of attack, and 0.1 psi dynamic pressure.

if, indeed, a significant computational cost savings is always achieved. In some cases, it is quite feasible that a combined solution may require fewer time steps than the individual time steps required for separate static and dynamic solutions. One possible strategy may be to initially perform a combined solution at a given dynamic pressure in order to get a sense of the static and dynamic properties of the configuration of interest. Based on that result, one might be able to make better decisions regarding the computational costs associated with performing separate static and dynamic solutions.

Previous ROM Approach

To date, the system-identification, time-domain-based methods for generating unsteady aerodynamic ROMs have relied on the traditional approach of separate and serial static and dynamic aeroelastic solutions presented above. For some methods,[1,6] the configuration investigated did not involve any static aeroelastic deformation. This is true for the AGARD 445.6 Wing which has a symmetric airfoil shape and, at zero degrees angle of attack, does not induce any static aeroelastic deformation. For other methods,[4] where the configuration induced a static aeroelastic effect, the unsteady aerodynamic ROM was generated about a converged static aeroelastic solution. That is, the ROM was generated using the initial conditions (restart) resulting from the converged static aeroelastic solution. This implies that the ROM was generated at the dynamic pressure at which the static aeroelastic solution was computed. Variation of the dynamic pressure via the ROM (which is how the ROM is used to explore the dynamic pressure solution space) then im-

plies ROM solutions that are removed from the static aeroelastic condition about which the ROM was originally generated. It is reasonable to expect that the accuracy of the ROM generated in this fashion will diminish the greater the difference between the dynamic pressure at which the ROM was generated and the dynamic pressure at which a ROM solution is desired.

Enhanced ROM Approach

For realistic configurations, the issue of static aeroelastic effects must be included in any ROM development. Because the accepted process used to generate ROMs was based on generating the ROM about a converged static aeroelastic solution, it was assumed that ROMs could not be used to compute static aeroelastic solutions. To date, no method had been identified for using a ROM for computing static aeroelastic solutions.

Careful analysis of the traditional approach for computing the separate and serial static and dynamic aeroelastic solutions indicates that the only parameters that vary from one solution (the static solution) to the next (the dynamic solution) are associated with the structure. That is, to compute a static aeroelastic solution, the modal damping is set to a very high value (0.99) and the structural initial conditions are set to zero. Then, to compute the dynamic aeroelastic response (restarted from the static aeroelastic solution), the modal damping is set to zero (or a small value) and the structural initial conditions (generalized velocities) are set to a small non-zero value. Therefore, if only a variation in structural parameters differentiate a static from a dynamic solution, the unsteady aerodynamic system used for both solutions is clearly identical. Following that thought, then, if an unsteady aerodynamic ROM can be used to predict dynamic aeroelastic responses (which comprises all of the system-identification, time-domain-based ROM results to date), surely that same unsteady aerodynamic ROM can be used to predict static aeroelastic responses. The first conclusion, then, is that the unsteady aerodynamic ROM should not be generated about a static aeroelastic solution as that negates the whole point of using unsteady aerodynamic ROMs for computing static aeroelastic solutions. The unsteady aerodynamic ROM must therefore be generated from the steady, rigid solution.

The next step is to understand how a static aeroelastic effect is induced within the CFL3D code (or any aeroelastic CFD code) and how that effect can be simulated using an unsteady aerodynamic ROM. The answer becomes clear when we consider two airfoils: a symmetric airfoil at zero degrees angle of attack and a nonsymmetric airfoil at any angle of attack. For a symmetric airfoil at zero degrees angle of attack, the pressures on the lower surface are identical to the pressures on the upper surface resulting in a zero net pressure difference. Since it is the pressure difference that is integrated with each mode shape to yield the generalized forces, the symmetric airfoil at zero degrees angle of attack, without any structural perturbation, does not generate any initial generalized forces. On the other hand, the nonsymmetric airfoil will induce a non-zero pressure difference which is then integrated with each mode shape to yield non-zero, initial generalized aerodynamic forces (GAFs). Therefore, it is this aerodynamic initial condition, consisting of non-zero GAFs, that is responsible for initiating (and perpetuating) a static aeroelastic response.

Figure 22 contains a schematic of the SIMULINK system used for predicting dynamic aeroelastic responses. The unsteady aerodynamic ROM (shown as the Discrete State-Space Model of Aerodynamics) was generated in one of two ways: 1). about a steady, rigid solution for a configuration without static aeroelastic effects or 2). about a converged static aeroelastic solution for a configuration with static aeroelastic effects.

In order to simulate static aeroelastic effects, the initial GAFs (induced by non-zero pressure difference on wing) are treated as a bias that is added to the unsteady aerodynamic ROM. The resultant SIMULINK model is presented as Figure 23. Note that the unsteady aerodynamic ROM shown in Figure 23 was generated about the steady, rigid solution. The initial values of GAFs shown in the stacked boxes in Figure 23 were obtained from the first time step of an aeroelastic solution at a selected dynamic pressure. By selecting these values from the solution at a given dynamic pressure, there still exists some limitation of how far the ROM can be exercised in terms of dynamic pressure. However, generating these initial GAFs at different dynamic pressures is computationally inexpensive. There is a computational cost savings from not having to execute a full static aeroelastic solution.

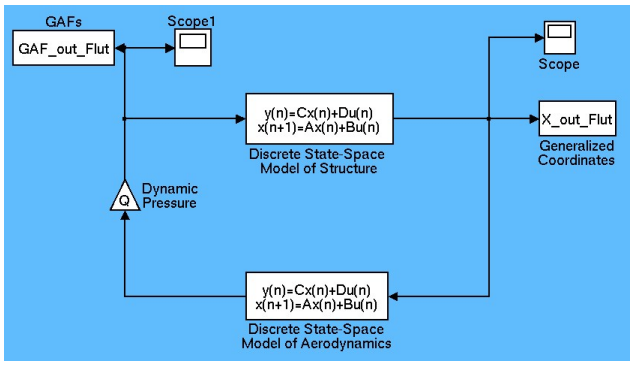

Fig. 22 SIMULINK model used for predicting dynamic aeroelastic responses only.

Another important point to make is with regards to

the level of excitation used to generate an unsteady aerodynamic ROM. In the previous method, where a ROM is generated about a converged static aeroelastic solution (i.e., a particular dynamic pressure), the selection of the dynamic pressure defines a region of aeroelastic behavior that is of interest. For example, if it is expected that the unsteady flow field will vary significantly beyond some elastic deformation of the structure, that elastic deformation corresponds to some value of dynamic pressure. The desired ROM can then be generated about that condition in order to capture important unsteady aerodynamic effects. With the new method for generating ROMs, since the unsteady aerodynamic ROM is generated from a steady, rigid solution, it is independent of dynamic pressure. With the new method, instead of using dynamic pressure to excite a particular range of unsteady aerodynamic behavior, it is the magnitude of the generalized coordinates (used as input to the unsteady aerodynamic system to define the ROM) that defines a particular region of interest.

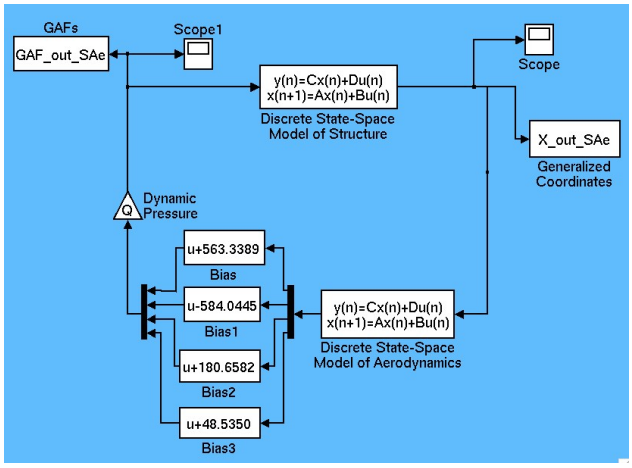

Fig. 23 SIMULINK model used for predicting both or either static and dynamic aeroelastic responses.

Comparison of various CFL3D and ROM static, dynamic, and combined aeroelastic responses are now presented. In another paper,[5] three new orthogonal functions are introduced that can be used to simultaneously excite all the modes of an unsteady aerodynamic system in order to generate an unsteady aerodynamic ROM with a single CFD execution. For the results that follow, the unsteady aerodynamic ROM was generated using the Walsh functions.[5]

The computation of static aeroelastic results using the ROM requires the modification of the modal damping within the state-space model of the structure presented in Figure 23. The modal damping for the structural state-space model is set to 0.99 and the initial conditions (also of the structure) are set to zero. A comparison of the static aeroelastic results computed using CFL3D already presented in Figure 18 and those computed using the ROM at a dynamic pressure of 0.1 psi is presented in Figure 24. The results compare very well, with a slight mismatch of the static aeroelastic response for the first generalized coordinate. This mismatch may be due to the selection of various parameters within the system identification process used to generate the ROM.

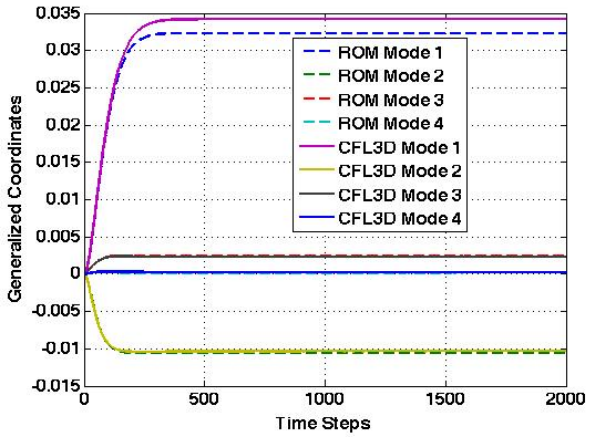

Fig. 24 Comparison of CFL3D and ROM static aeroelastic responses for the RSM configuration at 0.7 Mach number, 3 degrees angle of attack, and 0.1 psi dynamic pressure.

The same ROM configuration presented in Figure 23 can now be used to compute a combined static and dynamic aeroelastic solution at the same dynamic pressure. The modal damping of the structure is now set to zero and the initial conditions are set to the same values used in the CFL3D solution (generalized velocities equal to 0.001). Then the ROM solution is computed and the result is presented in Figure 25.

It can be seen that the comparison between the CFL3D (Figure 21) and ROM combined (static and dynamic) aeroelastic solutions is very good. The comparison of these responses for the first mode is presented as Figure 26.

The comparison of combined solutions for CFL3D and ROM for a dynamic pressure of 0.5 psi is presented in Figure 27. A discrepancy is noticed with respect to the static aeroelastic values and increased damping for the ROM solutions. Again, this discrepancy may be due to the particular set of parameters used within the system identification techniques to generate the ROM.

A comparison of only the dynamic portions of these responses is presented in Figure 28. This comparison has benefitted from the removal of the static aeroelatic effect. However, additional analyses are required to fully understand the source of some of these discrepancies.

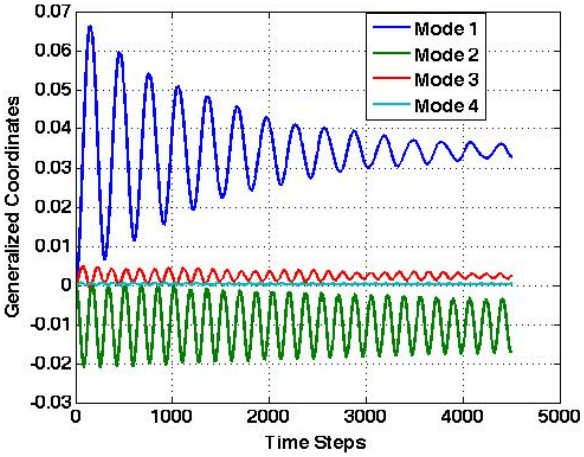

Fig. 25 Combined ROM static and dynamic aeroelastic solutions for the RSM configuration at 0.7 Mach number, 3 degrees angle of attack, and 0.1 psi dynamic pressure.

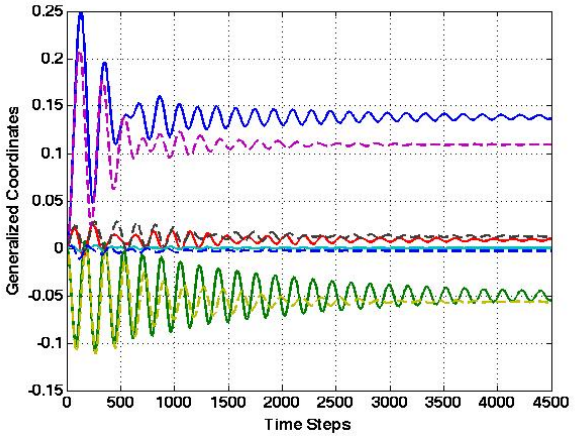

Fig. 27 Comparison of CFL3D (solid lines) and ROM (dashed lines) combined aeroelastic responses for the RSM configuration at 0.7 Mach number, 3 degrees angle of attack, and 0.5 psi dynamic pressure.

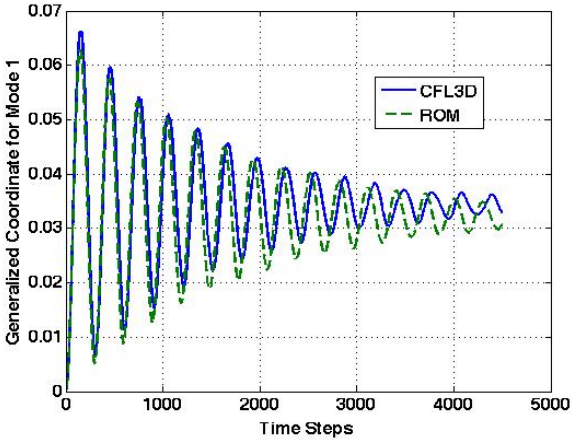

Fig. 26 Comparison of CFL3D and ROM combined aeroelastic response for the first mode for the RSM configuration at 0.7 Mach number, 3 degrees angle of attack, and 0.1 psi dynamic pressure.

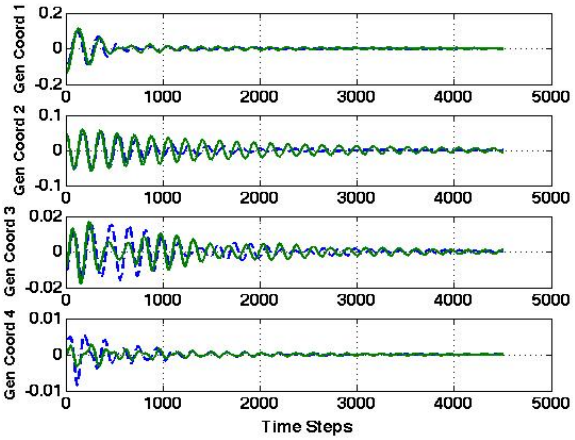

Fig. 28 Comparison of CFL3D (solid green line) and ROM (dashed blue line) dynamic aeroelastic responses for all four generalized coordinates for the RSM configuration at 0.7 Mach number, 3 degrees angle of attack, and 0.5 psi dynamic pressure.

Finally, a comparison of CFL3D and ROM dynamic aeroelastic responses at a dynamic pressure of 0.9 psi is presented in Figure 29. Although there exist some differences between some of the generalized coordinate responses, both the CFL3D and ROM solutions are at or near flutter.

This enhanced method shows promise towards the use of ROMs for full static and dynamic aeroelastic responses required for realistic configurations. In addition, subsequent research will investigate the effects of the different input functions (used to generate a ROM), input amplitudes, record length, and various SOCIT processing options on the aeroelastic responses using unsteady aerodynamic ROMs.

Matched-Point CFD-Based Analyses

Example Configuration-AGARD 445.6 Aeroelastic Wing

For the discussion regarding the ROM-based matched-point solution method, a CFL3D model of the AGARD 445.6 Aeroelastic Wing is used. The AGARD 445.6 Aeroelastic Wing has been used extensively by several authors to validate computational methods.[19–21] Although the aeroelastic behavior of this wing is fairly benign (weakly nonlinear), the aeroelastic data from the flutter test of this wing provides a good starting point for validation of computational techniques.[22] The wing is a 45-degree swept-back wing

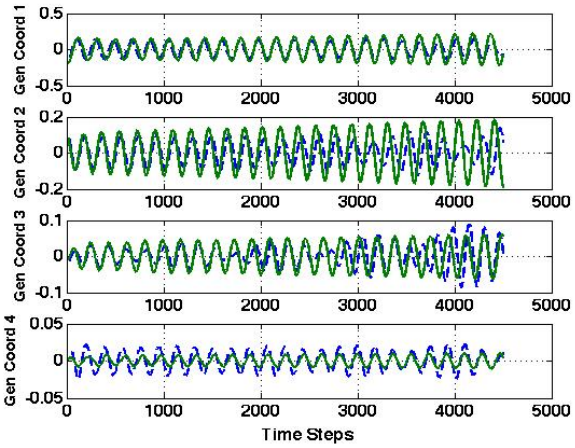

Fig. 29 Comparison of CFL3D (solid green line) and ROM (dashed blue line) dynamic aeroelastic responses for all four generalized coordinates for the RSM configuration at 0.7 Mach number, 3 degrees angle of attack, and 0.9 psi dynamic pressure.

with a NACA 65A004 airfoil section, panel aspect ratio of 1.65, and a taper ratio of 0.6576. Results presented are for Euler solutions using the grid presented as Figure 30. Additional details regarding this wing can be found in the references.

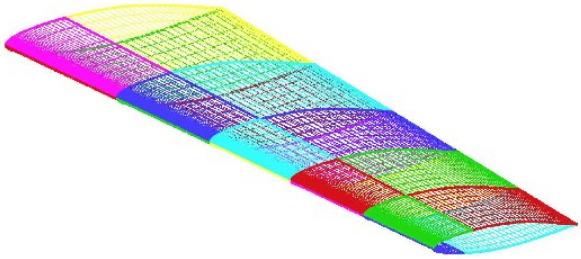

Fig. 30 CFL3D grid for AGARD 445.6 Aeroelastic Wing.

Traditional Approach

Another recent enhancement to the ROM methodology involves the use of a single ROM to compute matched-point solutions. Typically, for realistic configurations that fly in the atmosphere, it is important to understand the aeroelastic response of that vehicle at the corresponding atmospheric conditions. That is, a given altitude and Mach number define a particular dynamic pressure. This is referred to as a matched-point solution.

When performing aeroelastic CFD analyses, a matched-point solution is obtained by setting the Mach number, velocity, and dynamic pressure of interest. These three parameters together define a particular flight condition. As discussed above, an unsteady aerodynamic ROM is defined based on dynamic pressure variations; changes in dynamic pressure is also how the ROM is typically used for predicting aeroelastic responses. If a different matched-point solution is desired, this requires a re-execution of the CFD code at the new conditions (Mach number, dynamic pressure, and velocity). But a ROM, as discussed above, only captures the effect of dynamic pressure variations since, during the identification process, the velocity is kept constant. Different matched-point solutions would imply the need for different ROMs for the different conditions.

Enhanced ROM Approach

In order to minimize computational cost, it would be beneficial if a given unsteady aerodynamic ROM could be used to predict aeroelastic responses at any dynamic pressure and velocity. This issue involves understanding how velocity enters the aeroelastic equations of motion within an aeroelastic CFD solver.

The answer to this issue lies in the discretization of the equations, in particular, the definition of the time step used in the CFD solution. The equation for the actual (dimensional) time step is

$$dtact = \{dt * Machnumber * rlength/velocity\} \quad (4)$$

with dt being the non-dimensional time step and rlength is a reference length. Therefore, within an aeroelastic CFD solver, the effect of velocity is to alter the time step of numerical integration. With this in mind, a matched-point solution can be realized using a single unsteady aerodynamic ROM by simply modifying the sampling rate of the discrete state-space models shown in Figure 23 (aerodynamic and structural) such that the new sampling rate corresponds to the time step associated with a particular velocity back in the CFD code. Kim et al[4] introduce a similar concept but the present discretization is directly connected to the CFD time step (as defined within CFL3Dv6.4). The SIMULINK models require that the discrete time step associated with each system within the SIMULINK model (the aerodynamic and structural state-space systems) be the same or a multiple of the time step. Therefore, for a desired matched-point condition, both the aerodynamic and structural state-space models are re-sampled to the time step

consistent with the CFL3D time step. This is a very simple concept and the results are presented below.

Figure 31 presents a comparison of the generalized coordinate responses generated using a single unsteady aerodynamic ROM of the AGARD 445.6 Wing[1] at a dynamic pressure of 75 psf and a velocity of 973 ft/sec and the corresponding generalized coordinate responses from the direct CFL3D solution, both at M=0.9. These results were computed using the one-mode-at-a-time approach. Clearly, since the ROM used for this analysis was generated at this velocity, the comparison is excellent.

As stated above, the goal of the ROM matched-point solution technique is to be able to use a single unsteady aerodynamic ROM to predict the response of the aeroelastic system at various combinations of dynamic pressure and velocity in order to generate matched-point solutions. Defining a new time step based on a different velocity, a modified unsteady aerodynamic ROM and structural state-space model are generated using re-sampling techniques available in MATLAB. This is done by basically resampling the discrete-time systems at the new time step. Figure 32 presents a comparison of the generalized coordinate responses generated using a re-sampled version of the unsteady aerodynamic ROM at a dynamic pressure of 70 psf and a velocity of 400 ft/sec and the corresponding generalized coordinate responses from the direct CFL3D solution. As can be seen, the matched-point technique enables the use of a single unsteady aerodynamic ROM (although re-sampled to match velocity) to compute the response of the aeroelastic system to a variation in dynamic pressure and velocity.

Likewise, Figure 33 presents a comparison of the generalized coordinate responses generated at a dynamic pressure of 80 psf and a velocity of 1000 ft/sec and the corresponding generalized coordinate responses from the direct CFL3D solution. Once again, the comparison is excellent and serves to validate the newly-developed matched-point ROM solution.

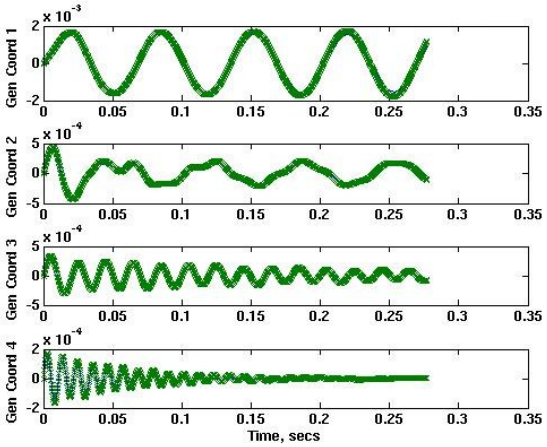

Fig. 31 Comparison of generalized coordinates from the ROM and the full CFL3D solution for the AGARD wing at M=0.9, Q=75 psf and U=973 ft/sec.

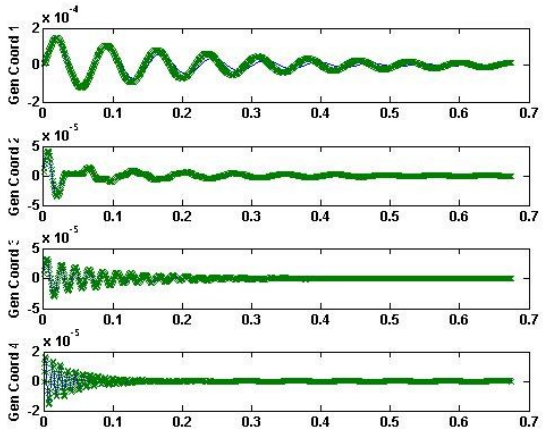

Fig. 32 Comparison of generalized coordinates from the ROM and the full CFL3D solution for the AGARD wing at M=0.9, Q=70 psf and U=400 ft/sec.

Concluding Remarks

Recent enhancements to the development of aeroelastic reduced-order models (ROMs) have been presented. These enhancements include the capability to compute combined static and dynamic aeroelastic responses and matched-point solutions using a single ROM. The simultaneous application of the structural modes as input to the CFD was briefly described as the details of this enhancement were provided in a separate paper. The ability to compute static and dynamic aeroelastic responses using the ROM was presented. Combined static and dynamic aeroelastic responses were computed using a ROM of the RSM supersonic configuration. These combined responses were compared with similar responses from the CFL3D code. The comparisons indicated reasonable correlation, depending on the dynamic pressure of interest. Additional research is underway to identify the source of some discrepancies as well as to optimize the overall process. Finally, the matched-point solution enhancement was shown to accurately compute aeroelastic responses of a given ROM of the AGARD 445.6 wing at various dynamic pressures and velocities. These new enhancements to the development of aeroelastic ROMs provides a significant advancement in ROM technology and enables the practical and efficient application of ROM technology to real-world problems.

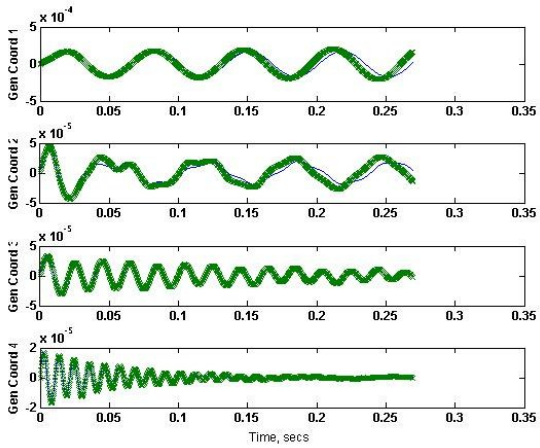

Fig. 33 Comparison of generalized coordinates from the ROM and the full CFL3D solution for the AGARD wing at M=0.9, Q=80 psf and U=1000 ft/sec.

References

[1]Silva, W. A. and Bartels, R. E., "Development of Reduced-Order Models for Aeroelastic Analysis and Flutter Prediction Using the CFL3Dv6.0 Code," *Journal of Fluids and Structures*, No. 19, 2004, pp. 729–745.

[2]Juang, J.-N. and Pappa, R. S., "An Eigensystem Realization Algorithm for Modal Parameter Identification and Model Reduction," *Journal of Guidance, Control, and Dynamics*, Vol. 8, 1985, pp. 620–627.

[3]"Registered Product of the MathWorks, Inc." .

[4]Kim, T., Hong, M., Bhatia, K. G., and SenGupta, G., "Aeroelastic Model Reduction for Affordable Computational Fluid Dynamics-Based Flutter Analysis," *AIAA Journal*, Vol. 43, 2005, pp. 2487–2495.

[5]Silva, W. A., "Simultaneous Excitation of Multiple-Input Multiple-Output CFD-Based Unsteady Aerodynamic Systems," *48th AIAA/ASME/ASCE/AHS/ASC Structures, Structural Dynamics, and Materials Conference*, No. AIAA Paper No. 2007-1988, Honolulu, HI, April 23-26 2007.

[6]Raveh, D. E., "Identification of Computational-Fluid-Dynamic Based Unsteady Aerodynamic Models for Aeroelastic Analysis," *Journal of Aircraft*, Vol. 41, June 2004, pp. 620–632.

[7]Krist, S. L., Biedron, R. T., and Rumsey, C. L., "CFL3D User's Manual Version 5.0," Tech. rep., NASA Langley Research Center, 1997.

[8]Bartels, R. E., "Mesh Strategies for Accurate Computations of Unsteady Spoiler and Aeroelastic Problems," *AIAA Journal of Aircraft*, Vol. 37, 2000, pp. 521–525.

[9]Bartels, R. E., Rumsey, C. L., and Biedron, R. T., "CFL3D Version 6.4: General Usage and Aeroelastic Analysis," *NASA TM 2006 214301*, April 2006.

[10]Roe, P. L., "Approximate Riemann Solvers, Parameter Vectors, and Difference Schemes," *Journal of Computational Physics*, Vol. 43, 1981, pp. 357–372.

[11]Juang, J.-N., Phan, M., Horta, L. G., and Longman, R. W., "Identification of Observer/Kalman Filter Markov Parameters: Theory and Experiments," *Journal of Guidance, Control, and Dynamics*, Vol. 16, 1993, pp. 320–329.

[12]Juang, J.-N., *Applied System Identification*, Prentice-Hall PTR, 1994.

[13]Silva, W. A., "Recent Enhancements to the Development of CFD-Based Aeroelastic Reduced Order Models," *48th AIAA/ASME/ASCE/AHS/ASC Structures, Structural Dynamics, and Materials Conference*, No. AIAA Paper No. 2007-2051, Honolulu, HI, April 23-26 2007.

[14]Eykhoff, P., *System Identification: Parameter and State Identification*, Wiley Publishers, 1974.

[15]Ljung, L., *System Identification: Theory for the User*, Prentice-Hall Publishers, 1999.

[16]Zhu, Y., *Multivariable System Identification for Process Control*, Pergamon Publishers, 2001.

[17]Hong, M., Kuruvila, G., Bhatia, K., SenGupta, G., and Kim, T., "Evaluation of CFL3D for Unsteady Pressure and Flutter Predictions," *44th AIAA/ASME/ASCE/AHS/ASC Structures, Structural Dynamics, and Materials Conference*, No. AIAA Paper No. 2003-1923, Norfolk, VA, April 7-10 2003.

[18]Silva, W. A. and Bennett, R. M., "Application of Transonic Small Disturbance Theory to the Active Flexible Wing Model," *Journal of Aircraft*, Vol. 32, 1995, pp. 16–22.

[19]Gordnier, R. E. and Melville, R. B., "Transonic Flutter Simulations Using an Implicit Aeroelastic Solver," *AIAA Journal of Aircraft*, Vol. 37, 2000, pp. 872–879.

[20]Gupta, K. K., Voelker, L. S., Bach, C., Doyle, T., and Hahn, E., "CFD-Based Aeroelastic Analysis of the X-43 Hypersonic Flight Vehicle," *Proceedings of the 39th Aerospace Sciences Meeting and Exhibit*, No. 2001-0712, Reno, CA, Jan. 2001.

[21]Lee-Rausch, E. M. and Batina, J. T., "Wing Flutter Computations Using an Aerodynamic Model Based on the Navier-Stokes Equations," *Journal of Aircraft*, Vol. 33, 1993, pp. 1139–1148.

[22]E. C. Yates, J., Land, N. S., and J. T. Foughner, J., "Measured and Calculated Subsonic and Transonic Flutter Characteristics of a 45-degree Swept-Back Wing Planform in Air and in Freon-12 in the Langley Transonic Dynamics Tunnel," Tech. rep., NASA, TN D-1616, 1963.